Title
GESFIDE-PROPELLER approach for simultaneous R2 and R2* measurements in the abdomen.

Journal
Magnetic resonance imaging, 31(10)

ISSN
0730-725X

Authors
Jin, Ning
Guo, Yang
Zhang, Zhuoli
et al.

Publication Date
2013-12-01

DOI
10.1016/j.mri.2013.08.003

Peer reviewed

Published in final edited form as:
Magn Reson Imaging. 2013 December ; 31(10): 1760–1765. doi:10.1016/j.mri.2013.08.003.

GESFIDE-PROPELLER Approach for Simultaneous R2 and R2* Measurements in the Abdomen

Ning Jin, PhD[1,2,3], **Yang Guo, MD**[2], **Zhuoli Zhang, MD, PhD**[2], **Longjiang Zhang, MD**[4], **Guangming Lu, MD**[5], and **Andrew C. Larson, Ph.D.**[1,2,5]

[1]Department of Biomedical Engineering, Northwestern University Chicago, Illinois, USA

[2]Department of Radiology, Northwestern University Chicago, Illinois, USA

[3]Siemens Medical Solutions USA, Inc., Chicago, Illinois, USA

[4]Department of Medical Imaging, Jinling Hospital, Clinical School of Medicine, Nanjing University, Nanjing, China

[5]Robert H. Lurie Comprehensive Cancer Center Chicago, Illinois, USA

Abstract

Purpose—To investigate the feasibility of combining GESFIDE with PROPELLER sampling approaches for simultaneous abdominal R2 and R2* mapping.

Materials and Methods—R2 and R2* measurements were performed in 9 healthy volunteers and phantoms using the GESFIDE-PROPELLER and the conventional Cartesian-sampling GESFIDE approaches.

Results—Images acquired with the GESFIDE-PROPELLER sequence effectively mitigated the respiratory motion artifacts, which were clearly evident in the images acquired using the conventional GESFIDE approach. There were no significant difference between GESFIDE-PROPELLER and reference MGRE R2* measurements ($p = 0.162$) whereas the Cartesian-sampling based GESFIDE methods significantly overestimated R2* values compared to MGRE measurements ($p < 0.001$).

Conclusion—The GESFIDE-PROPELLER sequence provided high quality images and accurate abdominal R2 and R2* maps while avoiding the motion artifacts common to the conventional Cartesian-sampling GESFIDE approaches.

Keywords

R2/R2* mapping; PROPELLER; GESFIDE; abdominal

Please send proof and correspondence to: Ning Jin, Ph.D., Siemens Healthcare, 460 W. 12th Ave., Room 311, Columbus, OH 43210, United States, Phone: 1-614-247-8794, ning.jin@siemens.com.

INTRODUCTION

Transverse relaxation serves as a critical contrast mechanism for a broad range of *in vivo* magnetic resonance imaging (MRI) applications. The intrinsic relaxation rate R2 (≡ 1/T2) is important for lesion detection and morphologic characterization during abdominal MRI scans; R2 can be measured using a series of single spin echoes images or, more conveniently, a series of multi-echo Carr-Purcell-Meiboom-Gill (CPMG) images (1). The effective transverse relaxation rate R2* (≡ 1/T2*) = R2 + R2′, with R2′ representing the reversible contribution to the total relaxation time. R2* can be derived from a series of T2*-weighted images sampled at increased echo formation times (TE). These images can be acquired using gradient-recall echo (2) or multiple gradient-recalled echo (MGRE) (3) pulse sequences.

R2 and R2* measurements have been combined to provide quantitative information descriptive of tissue hemodynamics. The ratio between R2 and R2* blood oxygenation level-dependent (BOLD) effects during hyperoxia and hypercapnia (ΔR2/ΔR2*) has been used as a biomarker to differentiate voxels containing large and small vessels (4). Recently, this work was extended to quantify blood volume and mean vessel sizes within brain tissues and assess tumor angiogenesis following infusion intravenous of superparamagnetic blood pool contrast agents (5-7). Furthermore, the simultaneous measurements of R2 and R2* could be used to quantitatively assess the biodistribution of holmium-loaded microspheres and investigate their use in selective internal radiation therapy of liver tumors (8). Alternatively, R2′ measurements (calculated as the difference between R2* and R2) have been used to non-invasively quantify altered iron content in the brain during neurodegenerative diseases (9), as well as in the liver and the heart in patients with thalassemia disease (10). R2′ measurements have also been used to evaluate cerebral and renal oxygenation (11,12) and remove non-susceptibility-based confounding contributions to blood oxygenation change estimates during reversible focal cerebral ischemia studies (13).

Given that R2 and R2* can be combined to provide diagnostic information, a sequence which allows efficient, simultaneous measurement of R2 and R2* may be particularly useful and practical. Ma and Wehrli developed the gradient echo sampling of the free induction decay (FID) and echo (GESFIDE) method for simultaneous R2 and R2* measurements (14); for GESFIDE the magnetization is sampled via multiple gradient echoes during the FID following a 90° excitation pulse and during spin rephasing following a 180° refocusing pulse. The magnetization decay during the FID yields the R2* measurement, while comparison of the amplitudes of the echoes at symmetric positions around the 180° refocusing pulse allow calculation of R2. The GESFIDE technique has been successfully applied for vessel size imaging (5), cerebral (15) and hepatic iron(10,16) quantification, holmium-loaded microsphere quantification (17) and the assessment of bone structure and function (18,19). Furthermore, this technique has great potential for accurate R2 measurement at ultrahigh field since it can overcome the effect of refocusing pulse errors by spoiling the transverse magnetization and analyzing the slope of FID and echoes (20). However, prior GESFIDE techniques utilized conventional Cartesian *k*-space sampling approaches; these spin-echo based R2 / R2* measurement methods may be particularly

challenging for abdominal applications due to respiratory, cardiovascular and visceral motion.

The PROPELLER (Periodically Rotated Overlapping ParallEL Lines with Enhanced Reconstruction) TSE sequence was previously introduced for T2-wieghted imaging and quantitative diffusion-weighted imaging with less sensitivity to motion artifacts due to intrinsic properties of oversampling in the center of *k*-space and the potential for segmental phase correction (21). Recently, the PROPELLER sequence was modified and optimized for quantitative T2 mapping in the abdomen (22). In this work, we developed a GESFIDE-PROPELLER sequence for simultaneous R2 and R2* measurements and performed both phantom and normal volunteer studies to demonstrate that the GESFIDE-PROPELLER approach enables the collection of accurate, high-quality R2 and R2* maps in the abdomen.

METHODS

GESFIDE-PROPELLER Sequence

The GESFIDE-PROPELLER sequence diagram is shown in Fig. 1. Two sets of gradient echoes with N echoes in each set were acquired symmetrically on both sides of the 180° refocusing pulse to sample FID and rephasing of the spin echo. Only echoes of equal polarity were collected to minimize the sensitivity to background field gradients. The voxel-wise magnitude of the signal as a function of time following the 90° excitation pulse is described as follows:

$$\mathrm{S}(\mathrm{t}) = \mathrm{S}_0 \cdot exp\left[-\left(\mathrm{R2}+\mathrm{R2}'\right)\cdot \mathrm{t}\right] \quad [1]$$

for FID portion (t<TE/2), and

$$\mathrm{S}(\mathrm{t}) = \mathrm{S}_0 \cdot exp\left[-\left(\mathrm{R2}-\mathrm{R2}'\right)\cdot \mathrm{t}\right] \cdot exp\left(-\mathrm{R2}'\cdot TE\right) \quad [2]$$

for rephasing portion (t>TE/2).

The GESFIDE-PROPELLER sequence acquires *k*-space data as blades rather than in a rectilinear Cartesian trajectory. Unlike the conventional PROPELLER sequence (21), which acquires an entire blade with multiple echoes during each repetition time (TR), no phase-encoding gradients were applied between gradient echoes in the GESFIDE-PROPELLER sequence in order to place the echoes at the same phase-encoding position for each sampled line during a single TR. Thus, the number of repetitions required to provide complete k-space coverage equals the number of the echoes in each TR × the total number of blades (NBL). For each echo time, a separate image was reconstructed, resulting in a total of 2×N (N = the number of the echoes in each gradient echo set) images from each acquisition.

Phantom Study

All experiments were performed using a 1.5T clinical MRI scanner (Magnetom Espree, Siemens Medical Solutions, Erlangen, Germany). A body matrix array coil and spinal array were used for signal reception. 10 agarose gel phantoms were constructed with Falcon®

tubes containing either 0, 1, 3, 5, 7, 15, 30, 60, 120, 250 or 350 mg samples of SPIO-containing glass microspheres (~50k spheres/mg) to produce different R2 and R2* values. Imaging parameters for the GESFIDE-PROPELLER sequence were: FOV = 200 × 200 mm^2, matrix = 128 × 128, TR = 2000 ms, the number of the echoes in each TR = 40, NBL = 6, BW = 600 Hz/pixel, echo spacing (ES) = 3 ms, slice thickness = 5 mm, two sets of 8 gradient echoes were acquired on both sides of the refocusing pulse. Imaging time = NBL × the number of the echoes in each TR × TR = 480s. R2 and R2* reference standard measurements were performed using single-echo spin echo (SE) and multiple-gradient-recalled-echo (MGRE) sequences respectively. The imaging parameters for SE sequence were: field of view (FOV) = 200 × 200 mm^2, matrix = 128 × 128, TR = 2000 ms, TE = 10, 20, 30, 40, 50, 60, 70, 100 ms, Bandwidth (BW) = 600 Hz/pixel, slice thickness = 5 mm. The imaging parameters for MGRE sequence were: FOV = 200 × 200 mm^2, matrix = 128 × 128, TR = 200 ms, echo train length (ETL) = 12, ES = 3 ms, which was matched to the ES of the GESFIDE-PROPELLER sequence, BW = 600 Hz/pixel.

Volunteer studies

Nine healthy volunteers were enrolled in this IRB-approved study; informed consent was obtained from each volunteer. A body matrix array coil and spinal array were used for signal reception. Abdominal GESFIDE-PROPELLER images were acquired with imaging parameters similar to prior phantom studies, but included FOV = 350 × 350 mm^2, spatial resolution = 2.7 × 2.7 × 5 mm^3, ES = 2.5 ms. All images were acquired during free-breathing using respiratory bellows triggering with TR = respiratory cycle which was different for each individual volunteer (3000 – 4000 ms). A frequency-selective fat saturation pulse was applied before each excitation pulse to reduce streaking artifacts caused by off-resonant fat signals. Translation, rotation and through-plane motion corrections were not used during the PROPELLER image reconstruction process for this study (given that each *k*-space blade segment was not acquired during a single TR but over multiple TRs). The conventional Cartesian-sampling GESFIDE sequence was also implemented; for each study this sequence was used to collect comparison images at the same slice positions with similar imaging parameters. For reference normal volunteer R2* measurements, another set of MGRE images were acquired during breath holding with the following parameters: FOV = 350 × 262 mm^2, matrix = 128 × 96, TR = 200 ms, BW = 600 Hz/pixel, ETL = 8, ES = 2.53 ms, total breath hold duration = 20 s.

In an additional healthy volunteer, we also acquired two sets of non-gated GESFIDE-PROPELLER images during free-breathing to qualitatively examine respiratory triggering effects. The imaging parameters were similar to respiratory-triggered GESFIDE-PROPELLER sequence with TR = 2000 ms. Two separate datasets were acquired, the first with 100% (NBL = 6) blade coverage and the second with 400% (NBL = 24) blade coverage (essentially using identical resolution and FOV but vastly oversampling PROPELLER *k*-space to examine signal averaging effects during free-breathing).

Data Analysis

For images acquired using GESFIDE-PROPELLER and the Cartesian-sampling GESFIDE sequences, voxel-wise R2* (≡ R2 + R2′) and $R2^-$ (≡ R2 - R2′) maps were measured by

employing the non-linear Levenberg-Marquardt algorithm to fit the mono-exponential function in Eqs. (1) and (2). R2 were calculated by averaging R2* and $R2^{-}$. Reference standard R2 and R2* measurements were derived from SE and MGRE images by fitting the mono-exponential function $S(TE_i) = S(0)\cdot\exp(-R2\cdot TE_i)$ and $S(TE_i) = S(0)\cdot\exp(-R2^{*}\cdot TE_i)$, where $S(TE_i)$ is the MR signal intensity at TE_i. For all the images, noise was estimated in the region of air without noticeable artifacts. Image data with signal intensity below twice the noise level was excluded from the fitting to reduce the possible influence of Rician distributed noise on the magnitude signal (23). For the phantom study, mean R2 and R2* acquired using GESFIDE-PROPELLER were measured for each vial and compared with the reference standards. In the volunteer abdominal studies, ROIs were placed in the liver parenchyma excluding blood vessels to measure the mean R2 and R2* within the liver. Comparisons between the mean R2* measured with MGRE during breath hold, and both GESFIDE-PROPELLER and Cartesian-sampling GESFIDE approaches during free-breathing were performed with linear regression analysis. For each volunteer, mean R2* measured using GESFIDE-PROPELLER and Cartesian-sampling GESFIDE approaches were compared with the corresponding MGRE measurements using pair-wise Student's *t*-test with significance level of 0.05. Mean liver R2 values acquired using GESFIDE-PROPELLER were also compared with the Cartesian-sampling GESFIDE results using pair-wise Student's *t*-test.

Image Quality Analysis

Qualitative comparisons were made between images acquired using GESFIDE-PROPELLER and Cartesian-sampling GESFIDE sequences to evaluate the effectiveness of PROPELLER sampling to reduce motion artifacts during abdominal imaging. GESFIDE images acquired at the 1st echo, 8th echo and 16th echo using the two techniques were displayed simultaneously along two rows. The order of display was randomized with regard to the acquisition techniques. Two experienced radiologists (with >10 years combined experience reading abdominal MRI) blinded to the image acquisition strategy scored the images together by consensus. A scoring system (1 - 4) was designed to evaluate image quality based on the artifact level: "1" indicated poor (severe artifacts obstructing visualization of organs and precluding interpretation); "2" indicated acceptable (many artifacts limiting interpretation); "3" indicated good (artifacts present but limited bearing upon interpretation); "4" excellent (no apparent artifacts). The scores for GESFIDE-PROPELLER and Cartesian-sampling GESFIDE methods were compared using pair-wise Wilcoxon signed rank tests with a significance level of 0.05.

RESULTS

The mean R2 and R2* within the phantoms measured using the GESFIDE-PROPELLER technique strongly correlated with the SE and MGRE reference standards with the correlation coefficients (r^2) = 0.992 and 0.998 respectively (Fig. 2).

Representative abdominal GESFIDE images acquired at the 1st echo, 8th echo and 16th echo using Cartesian-sampling GESFIDE and GESFIDE-PROPELLER sequences are shown in Fig. 3. The corresponding R2 and R2* maps for both imaging strategies are also shown.

Artifacts were evident in the images acquired using the conventional Cartesian-sampling GESFIDE technique, while there were no apparent motion artifacts or blurring observed in the GESFIDE-PROPELLER images, with abdominal organs and anatomical structures clearly delineated. Compared with the reference standard R2* map acquired using MGRE during breath-holding (Fig. 3c), the abdominal R2* measured using the Cartesian-sampling GESFIDE method was significantly overestimated due to respiratory motion. Motion artifacts were also observed in the R2 map measured using the Cartesian-sampling GESFIDE method. These findings were supported by the qualitative image scoring provided the blinded review process. Image quality scores for GESFIDE-PROPELLER and Cartesian-sampling GESFIDE were 3.77 ± 0.44 and 2.22 ± 0.44, respectively. The image scores for GESFIDE-PROPELLER were significantly superior to the scores for the Cartesian-sampling GESFIDE for each volunteer study ($p<0.001$ for these paired comparisons).

For volunteer studies, liver R2* measurements were 35.5 ± 9.1 Hz using GESFIDE-PROPELLER, 45.9 ± 8.0 Hz using Cartesian-sampling GESFIDE and 35.0 ± 8.9 Hz using MGRE sequence during breath-holding. Liver R2 measurements were 25.3 ± 4.5 Hz using GESFIDE-PROPELLER and 25.0 ± 4.4 Hz using Cartesian-sampling GESFIDE. The mean liver R2* measurements using the GESFIDE-PROPELLER technique were strongly correlated with the reference standard ($r^2 = 0.989$), while a weaker correlation was observed between the R2* measurements using Cartesian-sampling based GESFIDE and the reference standard ($r^2 = 0.828$) (Figure. 3d). There were no significant difference between GESFIDE-PROPELLER and MGRE R2* measurements ($p = 0.162$) whereas the Cartesian-sampling based GESFIDE methods significantly overestimated R2* values compared to MGRE measurements ($p < 0.001$).

GESFIDE-PROPELLER images from the same volunteer in Fig. 3 during free-breathing without respiratory bellows triggering are shown in Fig. 4. With 100% blade coverage, streak artifacts are observed in these non-gated GESFIDE-PROPELLER images and corresponding R2* and R2 maps. With increased the blade coverage (400%), there were no clearly apparent coherent motion artifacts in the GESFIDE-PROPELLER images. Non-gated GESFIDE-PROPELLER R2 map with 400% blade coverage produced similar image quality and R2 values as the R2 map from GESFIDE-PROPELLER with respiratory bellows triggering (Fig. 3b.5). However, both abdominal R2* maps acquired using non-gated GESFIDE-PROPELLER sequence with 100% and 400% coverage overestimated R2* compared with the reference MGRE R2* maps (Fig. 3c).

DISCUSSION

GESFIDE techniques, which sample the FID after the 90° excitation pulse and signal rephasing after the 180° refocusing pulse, enable simultaneous R2 and R2* measurements. However, application for abdominal imaging may be problematic due to respiratory motion which can cause severe artifacts and subsequent parametric measurement errors. The principle aim of this study was to demonstrate the feasibility of combining GESFIDE with PROPELLER sampling approaches for simultaneous abdominal R2 and R2* mapping. We validated the efficacy of the proposed GESFIDE-PROPELLER approach in phantoms and

normal volunteers. In these initial studies, the GESFIDE-PROPELLER sequence provided high quality images and accurate abdominal R2 and R2* maps while avoiding the motion artifacts common to the conventional Cartesian-sampling GESFIDE approaches.

Respiratory motion produced severe artifacts in conventional Cartesian-sampling GESFIDE images and reduced measurement accuracy for both R2 and R2* relaxation rates. Commonly, breath-holding can be used for abdominal imaging to eliminate respiratory motion; however, breath-holding is not feasible for the acquisition of GESFIDE images due to the relatively long acquisitions times. Navigator-gated GESFIDE sequences have been developed and applied for liver and heart imaging (10). However, the navigator echo generates saturation bands or signal voids in the liver; these regions thus cannot be quantitatively analyzed. For these studies we used respiratory bellows methods for gating image acquisition. Combined with respiratory triggering, the proposed GESFIDE-PROPELLER methods effectively suppressed motion artifacts, producing superior image quality and more accurate parametric measurements. No inter-blade motion correction was performed in this study because each *k*-space segment was not acquired in a single-shot snapshot fashion (as with conventional PROPELLER methods); additionally, for the chosen axial imaging slices, in-plane motion correction would be ineffective given that the primary direction of respiratory liver motion in the liver is in the cranial-caudal orientation. Since the motion insensitivity of GESFIDE-PROPELLER is mostly from the oversampling in the center of the k-space, in the future it will be valuable and instructive compare GESFIDE-PROPELLER and radial sampling based GESFIDE approaches for the measurement accuracy of R2 and R2* relaxation rates.

We also performed an experiment in a single normal volunteer to compare gated and non-gated GESFIDE-PROPELLER R2 and R2* measurements in the abdomen; while further study is necessary to rigorously examine this scenario, this example suggests the necessity to use respiratory triggering for GESFIDE-PROPELLER image acquisition to achieve accurate R2* measurements. However, likely due to low-spatial frequency averaging effects, fewer artifacts were observed in these non-gated GESFIDE-PROPELLER images compared to gated Cartesian-sampling GESFIDE images. With the increased blade coverage, streaking artifacts were reduced in the GESFIDE-PROPELLER images, which is attributed to the rotational *k*-space oversampling permitted with the PROPELLER acquisition scheme. R2* was significantly overestimated in the liver with non-gated GESFIDE-PROPELLER with 100% and 400% blade coverage, while no artifacts were observed in the R2 map with 400% coverage, suggesting that R2* measurements are more sensitive to respiratory motion. Future studies are clearly warranted to systematically compare the accuracy of R2 and R2* measurements using non-gated and gated GESFIDE-PROPELLER sequence with different blade coverages.

Prior studies demonstrated a good agreement between the R2 and R2* rates measured with GESFIDE approach and the reference standards from single-echo SE sequences and MGRE sequence (10,14). For SE or MGRE sequences, more echoes generally yield superior measurement accuracy. However, this same trend is not necessarily true for the GESFIDE sequence, since R2* and $R2^{-}$ are calculated separately using echoes from both sides of the refocusing pulse thus signal may decay below the noise floor leading to inaccurate

representation of the associated decay envelope. With a larger number of echoes or a subject with long R2/R2* values, $R2^-$ inaccuracy may increase due to the low signal-noise-ratio (SNR) in the echoes acquired after the refocusing pulse. Earlier studies have shown TE can be optimized for GESFIDE by selecting a value of roughly twice the anticipated T2* (24). The GESFIDE sequence parameters may need to be further optimized for more accurate R2 and R2* measurements if initially anticipated relaxation values are significantly different than those ultimately observed. Moreover, to account for the rapid R2* decay, the echo spacing could be reduced by increasing the readout bandwidth and by using a bipolar readout to remove the flyback gradients between the echoes.

One limitation of this study was the relatively long imaging time because of *k*-space oversampling with PROPELLER acquisition scheme, resulting in 1.57 ($\pi/2$) times data acquisition redundancy compared with the conventional Cartesian-sampling GESFIDE sequence. Future sequence optimization could include parallel imaging techniques to reduce imaging time. Additionally, we assumed that the $R2'$ effect mainly arose from the microscopic field inhomogeneities leading to exponential R2* decay, but the exponential decay tended to be modulated by functions describing intravoxel dephasing in the existence of large macroscopic field inhomogeneities (25) and R2/R2* could be contaminated. In that case, intravoxel dephasing could be included in the fitting to increase R2/R2* measurement accuracy. In the current study, images were generally acquired from the well-shimmed regions of the abdomen, so non-exponential R2* decay was not a significant issue. Frequency-selective fat saturation pulse was applied before the excitation to suppress chemical-shift induced streaking artifacts. However, fat saturation methods can be relatively sensitive to B_0 and B_1 inhomogeneities, resulting in partial or failed fat suppression. Huo et al. (26) recently proposed another approach for the Turboprop-IDEAL sequence to reduce chemical-shift artifacts by acquiring blade-pairs for each blade with opposite readout directions; however, this approach increases the total imaging time by a factor of 2. Further investigations to compare and optimize fat signal suppression approaches for these PROPELLER-based GESFIDE methods could be valuable to improve image quality and R2/R2* measurement accuracy.

In conclusion, the GESFIDE-PROPELLER approach can simultaneously provide accurate R2 and R2* measurements in the abdomen. The proposed method can produce high quality images and accurate transverse relaxation measurements for a broad range of body imaging applications wherein conventional Cartesian-sampling approaches are particularly prone to failure.

REFERENCES

1. Carr HY, Purcell EM. Effects of Diffusion on Free Precession in Nuclear Magnetic Resonance Experiments. Phys Rev. 1954; 94:630–638.
2. Haacke EM, Hopkins A, Lai S, Buckley P, Friedman L, Meltzer H, Hedera P, Friedland R, Klein S, Thompson L, et al. 2D and 3D high resolution gradient echo functional imaging of the brain: venous contributions to signal in motor cortex studies. NMR Biomed. 1994; 7(1-2):54–62. [PubMed: 8068526]
3. Prasad PV, Chen Q, Goldfarb JW, Epstein FH, Edelman RR. Breath-hold R2* mapping with a multiple gradient-recalled echo sequence: application to the evaluation of intrarenal oxygenation. J Magn Reson Imaging. 1997; 7(6):1163–1165. [PubMed: 9400864]

4. Prinster A, Pierpaoli C, Turner R, Jezzard P. Simultaneous measurement of DeltaR2 and DeltaR2* in cat brain during hypoxia and hypercapnia. Neuroimage. 1997; 6(3):191–200. [PubMed: 9344823]
5. Tropres I, Grimault S, Vaeth A, Grillon E, Julien C, Payen JF, Lamalle L, Decorps M. Vessel size imaging. Magn Reson Med. 2001; 45(3):397–408. [PubMed: 11241696]
6. Tropres I, Lamalle L, Peoc'h M, Farion R, Usson Y, Decorps M, Remy C. In vivo assessment of tumoral angiogenesis. Magn Reson Med. 2004; 51(3):533–541. [PubMed: 15004795]
7. Ungersma SE, Pacheco G, Ho C, Yee SF, Ross J, van Bruggen N, Peale FV Jr. Ross S, Carano RA. Vessel imaging with viable tumor analysis for quantification of tumor angiogenesis. Magn Reson Med. 2010; 63(6):1637–1647. [PubMed: 20512867]
8. Seppenwoolde JH, Nijsen JF, Bartels LW, Zielhuis SW, van Het Schip AD, Bakker CJ. Internal radiation therapy of liver tumors: qualitative and quantitative magnetic resonance imaging of the biodistribution of holmium-loaded microspheres in animal models. Magn Reson Med. 2005; 53(1): 76–84. [PubMed: 15690505]
9. Haacke EM, Cheng NY, House MJ, Liu Q, Neelavalli J, Ogg RJ, Khan A, Ayaz M, Kirsch W, Obenaus A. Imaging iron stores in the brain using magnetic resonance imaging. Magn Reson Imaging. 2005; 23(1):1–25. [PubMed: 15733784]
10. Song R, Cohen AR, Song HK. Improved transverse relaxation rate measurement techniques for the assessment of hepatic and myocardial iron content. J Magn Reson Imaging. 2007; 26(1):208–214. [PubMed: 17659538]
11. Yang X, Cao J, Wang X, Li X, Xu Y, Jiang X. Evaluation of renal oxygenation in rat by using R2′ at 3-T magnetic resonance: initial observation. Acad Radiol. 2008; 15(7):912–918. [PubMed: 18572128]
12. Hoppel BE, Weisskoff RM, Thulborn KR, Moore JB, Kwong KK, Rosen BR. Measurement of regional blood oxygenation and cerebral hemodynamics. Magn Reson Med. 1993; 30(6):715–723. [PubMed: 8139453]
13. Grune M, van Dorsten FA, Schwindt W, Olah L, Hoehn M. Quantitative T*(2) and T'(2) maps during reversible focal cerebral ischemia in rats: separation of blood oxygenation from nonsusceptibility-based contributions. Magn Reson Med. 1999; 42(6):1027–1032. [PubMed: 10571923]
14. Ma J, Wehrli FW. Method for image-based measurement of the reversible and irreversible contribution to the transverse-relaxation rate. J Magn Reson B. 1996; 111(1):61–69. [PubMed: 8620286]
15. Hikita T, Abe K, Sakoda S, Tanaka H, Murase K, Fujita N. Determination of transverse relaxation rate for estimating iron deposits in central nervous system. Neurosci Res. 2005; 51(1):67–71. [PubMed: 15596242]
16. Song R, Lin W, Chen Q, Asakura T, Wehrli FW, Song HK. Relationships between MR transverse relaxation parameters R*(2), R(2) and R'(2) and hepatic iron content in thalassemic mice at 1.5 T and 3 T. NMR Biomed. 2008; 21(6):574–580. [PubMed: 18041805]
17. Seevinck PR, Seppenwoolde JH, Zwanenburg JJ, Nijsen JF, Bakker CJ. FID sampling superior to spin-echo sampling for T2*-based quantification of holmium-loaded microspheres: theory and experiment. Magn Reson Med. 2008; 60(6):1466–1476. [PubMed: 19026005]
18. Yablonskiy DA, Reinus WR, Stark H, Haacke EM. Quantitation of T2′ anisotropic effects on magnetic resonance bone mineral density measurement. Magn Reson Med. 1997; 37(2):214–221. [PubMed: 9001145]
19. Wehrli FW, Song HK, Saha PK, Wright AC. Quantitative MRI for the assessment of bone structure and function. NMR Biomed. 2006; 19(7):731–764. [PubMed: 17075953]
20. Cox EF, Gowland PA. Simultaneous quantification of T2 and T'2 using a combined gradient echo-spin echo sequence at ultrahigh field. Magn Reson Med. 2010; 64(5):1440–1445. [PubMed: 20593370]
21. Pipe JG. Motion correction with PROPELLER MRI: application to head motion and free-breathing cardiac imaging. Magn Reson Med. 1999; 42(5):963–969. [PubMed: 10542356]
22. Deng J, Larson AC. Modified PROPELLER approach for T2-mapping of the abdomen. Magn Reson Med. 2009; 61(6):1269–1278. [PubMed: 19353672]

23. Henkelman RM. Measurement of signal intensities in the presence of noise in MR images. Med Phys. 1985; 12(2):232–233. [PubMed: 4000083]

24. Song R, Song HK. Echo-spacing optimization for the simultaneous measurement of reversible ($R2'$) and irreversible (R2) transverse relaxation rates. Magn Reson Imaging. 2007; 25(1):63–68. [PubMed: 17222716]

25. Dahnke H, Schaeffter T. Limits of detection of SPIO at 3.0 T using T2 relaxometry. Magn Reson Med. 2005; 53(5):1202–1206. [PubMed: 15844156]

26. Huo D, Li Z, Aboussouan E, Karis JP, Pipe JG. Turboprop IDEAL: a motion-resistant fat-water separation technique. Magn Reson Med. 2009; 61(1):188–195. [PubMed: 19097201]

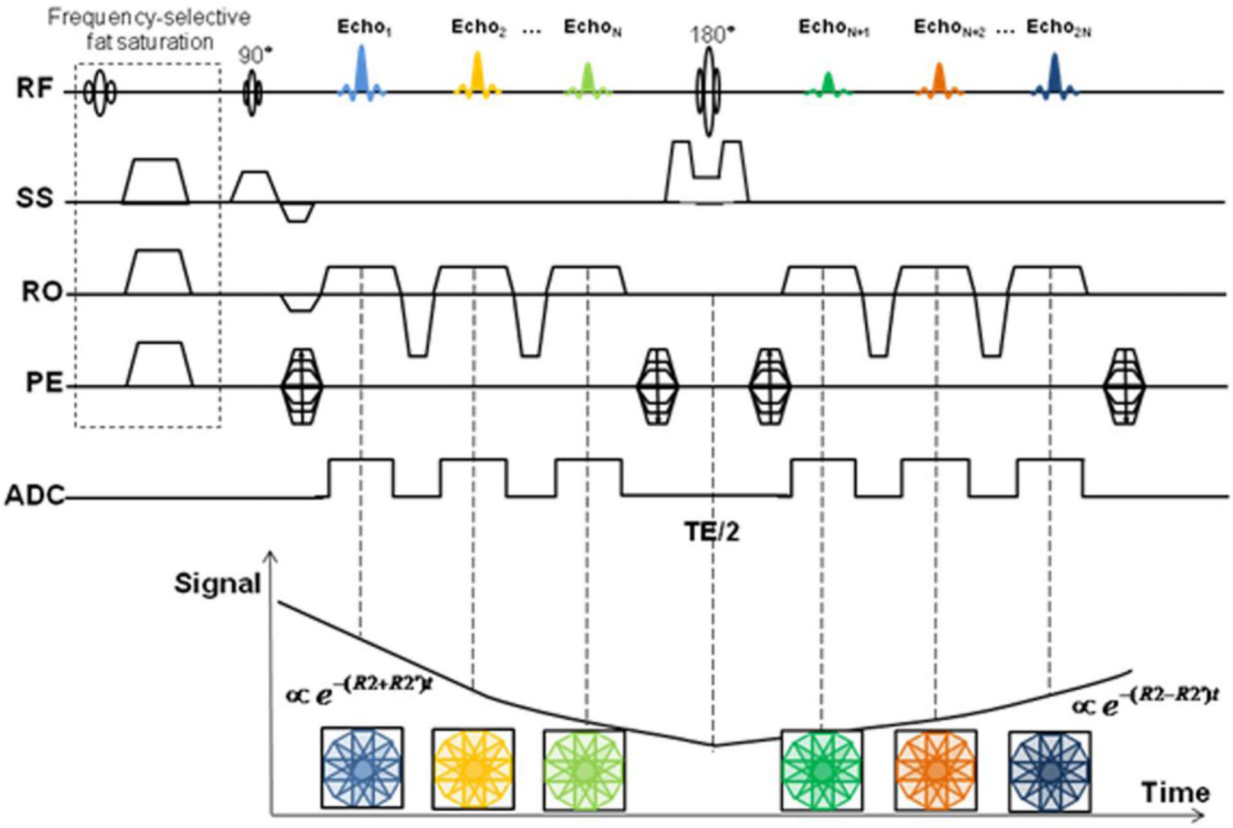

Figure 1.

GESFIDE-PROPELLER sequence diagram: Frequency-selective fat-saturation pulse was applied before the excitation. Two sets of N gradient echoes were acquired symmetrically on both side of the 180° refocusing pulse to sample FID and rephasing part of the spin echo. No phase-encoding gradients were applied between gradient echoes in the GESFIDE-PROPELLER sequence in order to place the echoes at the same phase-encode position. For each echo, a separate image was reconstructed resulting in a total of 2N images.

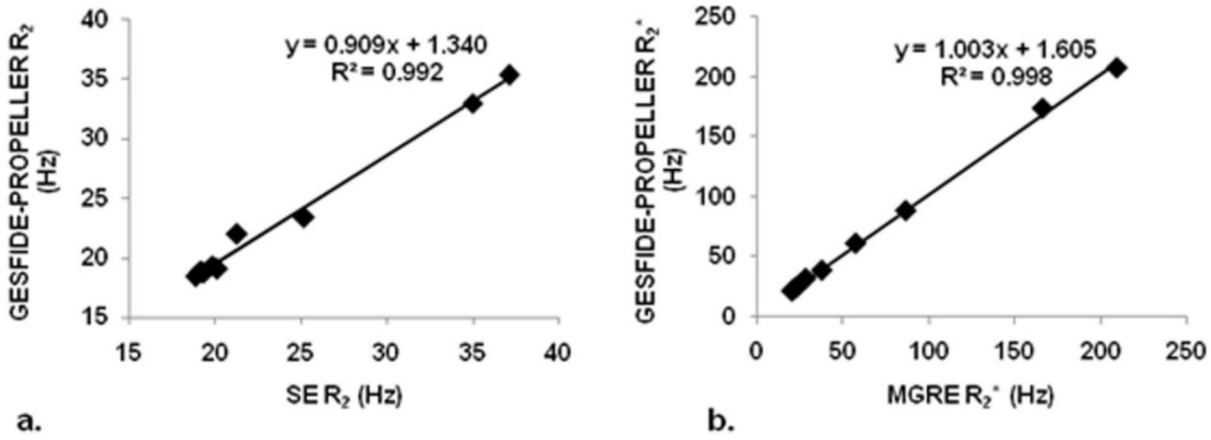

Figure 2.

GESFIDE-PROPELLER R2 and R2* measurements in phantom models were strongly correlated to reference standard SE and MGRE based measurements.

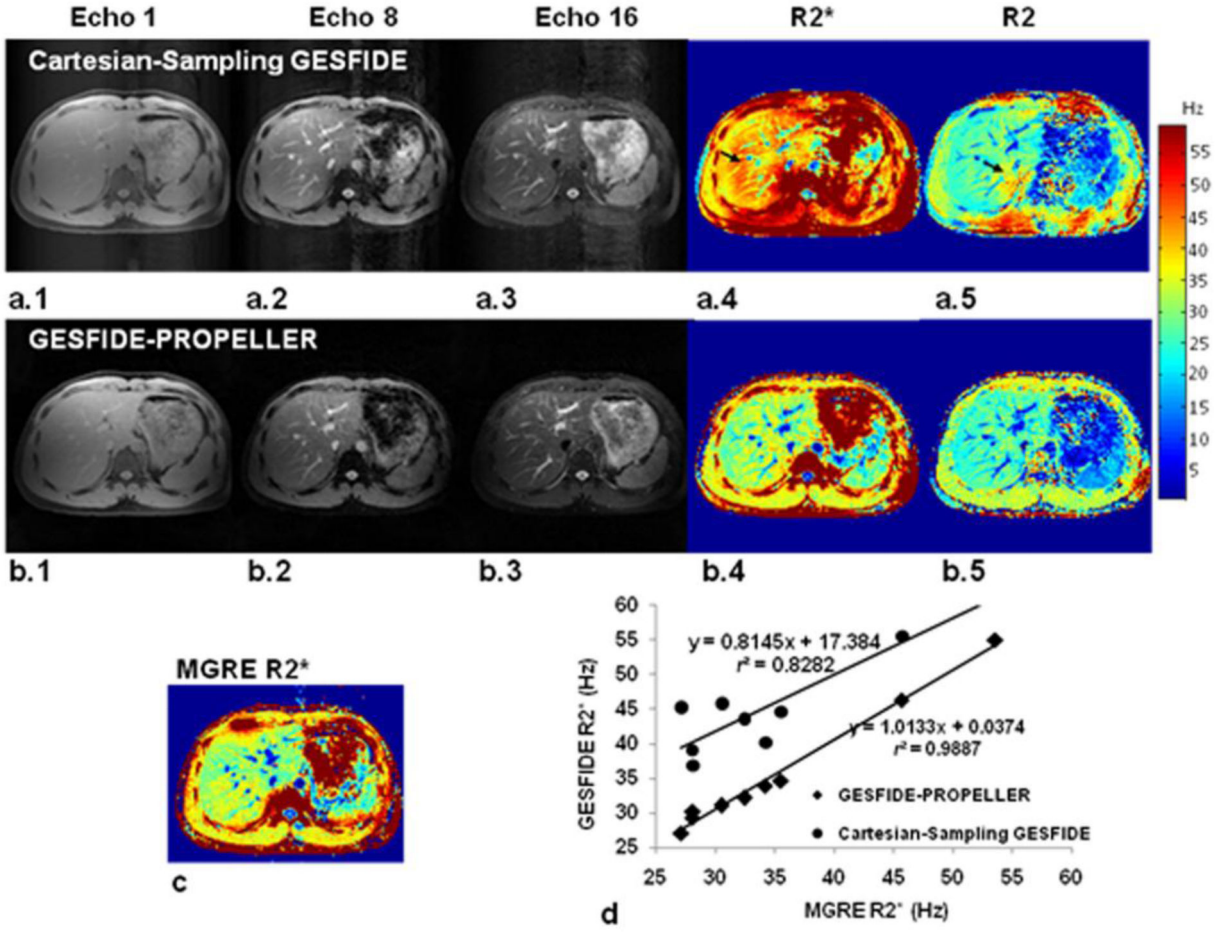

Figure 3.

GESFIDE images from the 1st (**Column 1**), 8th (**Column 2**) and 16th (**Column 3**) echoes and corresponding R2* (**Column 4**) and R2 (**Column 5**) maps from Cartesian-sampling GESFIDE (**a**) and GESFIDE-PROPELLER (**b**) sequences during free-breathing with respiratory bellows triggering. Artifacts (**arrows**) were observed in R2* and R2 maps measured using the Cartesian-sampling GESFIDE sequence. (**c**) Reference standard R2* map acquired using MGRE during breath holding. (**d**) R2* measurements in the liver acquired using the GESFIDE-PROPELLER technique were strongly correlated to reference standard MGRE measurements (r^2 = 0.989); Cartesian-sampling based GESFIDE measurements tended to overestimate liver R2* values.

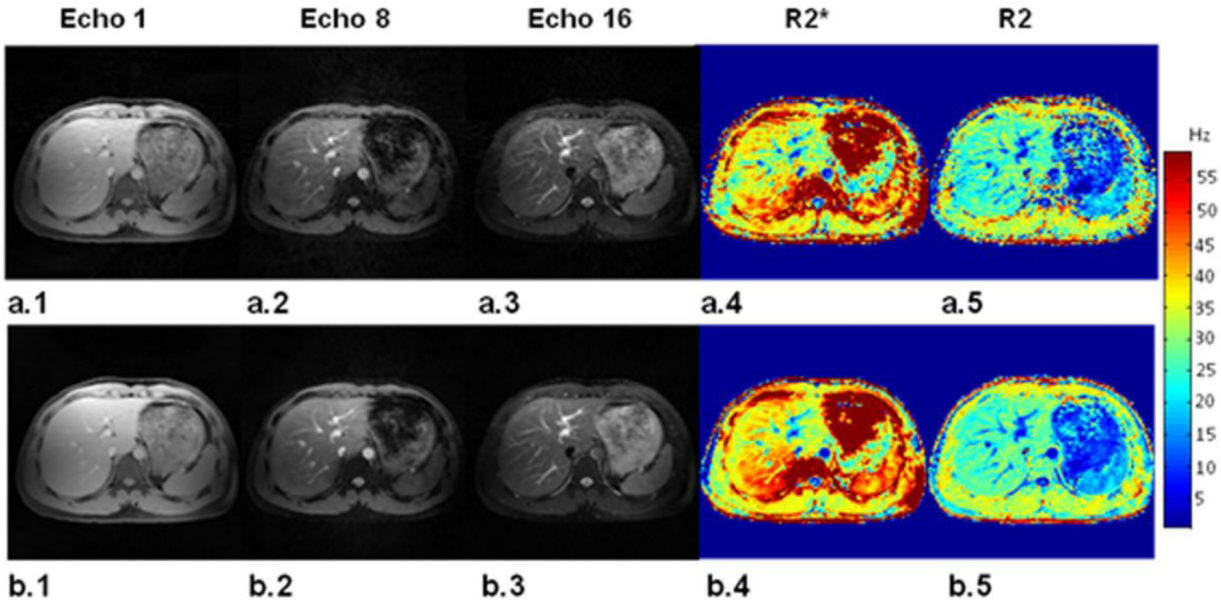

Figure 4.

GESFIDE images from the 1st (**Column 1**), 8th (**Column 2**) and 16th (**Column 3**) echoes and corresponding R2* (**Column 4**) and R2 (**Column 5**) maps from GESFIDE-PROPELLER sequences during free-breathing but without respiratory bellows triggering with 100% (**a**) and 400% (**b**) *k*-space blade coverage (same volunteer and slice position as Fig. 3).